frontiers | Frontiers in Genetics

TYPE Original Research
PUBLISHED 08 January 2024
DOI 10.3389/fgene.2023.1321379

OPEN ACCESS

EDITED BY
M. Kathryn Iovine,
Lehigh University, United States

REVIEWED BY
Kefei Li,
Cornell University, United States
Daniel Grimes,
University of Oregon, United States

*CORRESPONDENCE
Masakatsu Watanabe,
watanabe-m@fbs.osaka-u.ac.jp
Toshihiro Aramaki,
taramaki@fbs.osaka-u.ac.jp

†PRESENT ADDRESS
Toshihiro Aramaki,
Laboratory of Gene Regulation Research, Division of Biological Science, Graduate School of Science and Technology, Nara Institute of Science and Technology, Nara, Japan

RECEIVED 14 October 2023
ACCEPTED 20 December 2023
PUBLISHED 08 January 2024

CITATION
Ramli, Aramaki T, Watanabe M and Kondo S (2024), Piezo1 mutant zebrafish as a model of idiopathic scoliosis.
Front. Genet. 14:1321379.
doi: 10.3389/fgene.2023.1321379

Piezo1 mutant zebrafish as a model of idiopathic scoliosis

Ramli[1], Toshihiro Aramaki[1,2*†], Masakatsu Watanabe[1*] and Shigeru Kondo[1]

[1]Laboratory of Pattern Formation, Graduate School of Frontier Biosciences, Osaka University, Suita, Japan, [2]Japan Science and Technology Agency, PRESTO, Tokyo, Japan

Scoliosis is a condition where the spine curves sideways, unique to humans due to their upright posture. However, the cause of this disease is not well understood because it is challenging to find a model for experimentation. This study aimed to create a model for human idiopathic scoliosis by manipulating the function of mechanosensitive channels called Piezo channels in zebrafish. Zebrafish were chosen because they experience similar biomechanical forces to humans, particularly in relation to the role of mechanical force in scoliosis progression. Here we describe *piezo1* and *piezo2a* are involved in bone formation, with a double knockout resulting in congenital systemic malformations. However, an in-frame mutation of *piezo1* led to fully penetrant juvenile-onset scoliosis, bone asymmetry, reduced tissue mineral density, and abnormal intervertebral discs—resembling non-congenital scoliosis symptoms in humans. These findings suggest that functional Piezo channels responding to mechanical forces are crucial for bone formation and maintaining spine integrity, providing insights into skeletal disorders.

KEYWORDS

idiopathic scoliosis, Piezo channel, TMD, vertebral bone, zebrafish

1 Introduction

Scoliosis is a spinal deformity in which the spine curves sideways. It is estimated that approximately 5% of the world population is affected by scoliosis, the most common being idiopathic scoliosis that develops during adolescence (Konieczny et al., 2013). Various studies have linked the incidence of idiopathic scoliosis to central nervous system abnormalities (Burwell et al., 2009), hormonal imbalances (Kulis et al., 2015), muscle defects (Allam and Schwabe, 2013), and genetics (Wise et al., 2008), but details regarding the mechanisms of pathogenesis and other factors are not yet known.

One factor that has received attention as a possible cause of spinal deformity is mechanical forces (pressure and shear stress) (Hawes and O'brien, 2006). When the spine is subjected to unbalanced forces, the intervertebral discs are asymmetrically compressed and unequal growth of the spine occurs. This unequal spinal growth is thought to cause a positive feedback that results in a continual imbalance of mechanical loading, which ultimately inhibits spinal growth (Xie et al., 2022).

Animal models are commonly used to study pathology. However, in the case of scoliosis, the direction of gravity on the spine is different, making common animal models such as mice and rats unsuitable for research. In humans, due to the upright posture, the gravitational load is applied from a direction parallel to the spinal column (Castelein et al., 2005). In contrast, in quadrupedal animals, the direction of the vertebrae and the direction of gravity are perpendicular, so the contribution of gravity to bone growth

is quite different (Xie et al., 2022). Therefore, bipedal chicks have been tried as an animal model for scoliosis, but they are not a perfect model for the condition because their spinal columns are not as flexible as those of humans, limiting spinal flexion and extension (Fagan et al., 2009).

Interestingly, on the other hand, guppies, zebrafish, and medaka fish are known to spontaneously develop scoliosis. Fish are similar to humans in that during swimming, caudal propulsive forces cause the spine to compress in a direction similar to that of humans which may make fish susceptible to bone kinking (Gorman and Breden, 2009). Many studies have reported the usefulness of using zebrafish to understand the pathogenesis of scoliosis. For example, irregular cerebrospinal fluid flow caused by abnormal motile cilia can induce idiopathic scoliosis in zebrafish (Grimes et al., 2016; Zhang et al., 2018; Troutwine et al., 2020). Moreover, abnormal muscle fiber has been reported to develop notochord kinks that progress to scoliosis in zebrafish (Whittle et al., 2020). However, since mechanical loading is believed to contribute to scoliosis progression, it is necessary to establish an animal model that is suitable for this issue.

There are several genetic lineages in people presumed to be related to scoliosis, one of which is the mechanoreceptor Piezo channels. Piezo channels are located on the cell membrane and act as mechanotransducers. When physical forces are applied, Piezo channels are activated and cations such as calcium move into the cell, and activate several signaling pathways. There are two types of Piezo channels, Piezo1 and Piezo2 channels, which are encoded by the *piezo1* and *piezo2* genes, respectively. Piezo1 channel is highly expressed in non-sensory tissues such as the lung, skin, and bladder, unlike Piezo2, which is highly expressed in sensory tissues (Murthy et al., 2017).

It has been confirmed that *piezo1* genes are highly expressed in mesenchymal stem cells, osteoblasts, chondrocytes, and nucleus pulposus cells of intervertebral disc of the spine (Zhu et al., 2021). This underlines that *piezo1* might contribute to several bone metabolic and degenerative diseases such as osteoporosis, idiopathic scoliosis, or intervertebral disc degeneration. In a recent study, bipedal mice that suffered from scoliosis exhibited asymmetric *Piezo1* expression due to different compression stress of growth plate area. This will induce different degrees of apoptosis of chondrocyte as well as bone growth in growth plate that eventually lead to bone wedging. (Chen et al., 2023). Furthermore, another study demonstrated that patients with osteoporosis had significantly lower *PIEZO1* expression accompanied with low osteoblast marker genes (Sun et al., 2019). In addition, recent clinical report has revealed novel mutations in *PIEZO1* in patients with primary lymphatic dysplasia with symptoms of facial bone hypoplasia, thoracolumbar scoliosis, and short stature (Lee et al., 2021).

On the other hand, *PIEZO2* gene is important in proprioceptive function and is mainly expressed in muscle spindle and the Golgi tendon organ. One study reported that loss of *Piezo2* in the proprioceptive system induces abnormal alignment of spine and misshapen joint in mice (Assaraf et al., 2020). In human, mutation in this gene can lead to several skeletal abnormalities including arthrogryposis, spinal fusion, scoliosis, and hip dysplasia (Haliloglu et al., 2017; Uehara et al., 2020). Therefore, the abovementioned studies demonstrate the importance of Piezo channel in skeletal development.

In this study, we proposed that optimal sensing of mechanical force is crucial for the pathogenesis of scoliosis, not just the force itself. To investigate this, we disrupted the ability of zebrafish to sense mechanical force by knocking out *piezo* genes. Zebrafish have three *piezo* genes in their genome (*piezo1*, *piezo2a*, and *piezo2b*), and when we deleted both *piezo1* and *piezo2a* simultaneously or introduced an in-frame mutation of *piezo1*, the fish exhibited symptoms similar to bone diseases, including scoliosis and intervertebral disc degeneration. These findings indicate that zebrafish with deleted *piezo* genes could serve as an animal model for studying scoliosis. Our results provide valuable insights into the role of Piezo channels in bone development and may shed light on potential causes of skeletal disorders.

2 Material and methods

2.1 Zebrafish husbandry

All experiments in this study were conducted in accordance with the prescribed guidelines and approved protocols for the handling and use of animals at Osaka University. Tübingen (Tü) strain was used as the wildtype zebrafish and all fish were maintained under standard conditions. Fish were kept under a photoperiod of 14 h light/10 h darkness at 28 ^{O}C in a fish breeding room. Embryos were obtained by crossing mature males and females at 28 ^{O}C. Embryos were collected and incubated in a thermostatic incubator at 28.5 ^{O}C. After hatching, larvae were transferred to the fish breeding room and fed paramecia until they grew to be able to eat artificial diets.

2.2 CRISPR/Cas9

For generating zebrafish mutant, CRISPR/Cas9-mediated method was utilized. The sgRNA target site for each gene was designed using crisprscan.org. The sequences of the oligonucleotide for sgRNA are listed in Supplementary Table S1. To Knock-out *piezo1* and *piezo2a* gene, exon 5 of *piezo1* with target sequence 5′ CCTCAGGGTGTGCTG TGGCTCCT 3′ and exon 4 of *piezo2a* with target sequence 5′ TGG CCACGCTCATCCGCCTCTGG 3′ were chosen. For sgRNA transcription, the template DNA was made by polymerase chain reaction using oligonucleotide containing target exon and tracrRNA backbone. Then, about 50 ng synthesized template DNA was *in vitro* transcribed using *in vitro* Transcription T7 Kit (for siRNA Synthesis) (Takara bio), treated with DNase I (Takara Bio), and purified by RNA clean and concentration kit (Zymo Research).

To generate *piezo1* in-frame mutant, an effective single guide RNA (sgRNA) sequence for zebrafish *piezo1* had been reported previously (Gudipaty et al., 2017). This sgRNA targeted the splice acceptor sequence of exon 2 of zebrafish *piezo1* gene. The target sequence is 5′-cagCCTGCATATTTCGCTAC-3′ (exonic sequence is shown in uppercase, intronic sequence in lowercase). The 20 nucleotides sequence upstream of PAM were cloned into pDR274 plasmid containing RNA loop structure sequence required for recognition by Cas9 enzyme, and T7 promoter sequence that allowed for *in vitro* synthesis of sgRNA using MEGA Script T7 Kit (Invitrogen #AM1334). Synthesized sgRNA was mixed with Cas9 protein (NEB# M0646T) just before microinjection into zebrafish embryo.

2.3 Microinjection and genotyping

One-cell stage zebrafish embryos were injected with 1–2 nL of injection solution containing 300 ng/μL of Cas9 protein (NEB# M0646T) and 12.5 ng//μL of sgRNA. For genotyping, the DNA was extracted from embryos at 3 dpf or amputated caudal fin at adult stage. These samples then were incubated in DNA extraction buffer supplemented with Proteinase K at 55 ^{O}C for 2 h and 95 ^{O}C for 5 min. The extracted samples were diluted 300 times using distilled water and about 1 μL of diluted sample was used as a template for 20 μL standard PCR amplification. Primers for genotyping are listed in Supplementary Table S2.

2.4 Micro-CT

To analyze bone morphology and phenotypes in detail, utilize micro–computed tomography (micro-CT) is used. Whole-body fish was fixed in 4% PFA overnight. Fixed samples were observed by micro–CT-scanner SkyScan 1,172 (SkyScan NV, Aartselaar, Belgium) following the manufacturer's instructions. The X-ray source ranged from 50 kV, and the datasets were acquired at a resolution of 5 μm/pixel for abdominal or caudal part and 12 μm/pixel for whole body, depending on the size of each vertebral body. Samples were scanned in air dry condition. Neural arches and hemal arches were not included in bone analysis. After applying a fixed threshold for all samples, 3D evaluation is conducted using CTVox and CTAn. Orthoslice images were obtained using Dataviewer (Bruker, Kontich, Belgium).

2.5 Alizarin red S staining

For live imaging, fish at larvae (8 dpf), juvenile (20 dpf), and young adult (35 dpf) were incubated in 0.005% alizarin red S (Sigma) overnight and washed three times with tank water. Before observation, samples were anesthetized using *Ethyl 3-aminobenzoate methanesulfonate*. Imaging was performed on a BZ-X710 Keyence fluorescence microscope.

2.6 Histology and alkaline phosphatase staining

Since alkaline phosphatase is an enzymatic reaction, fixation and long incubation time in chemical solution will affect the result. To address this problem, we perform Kawamoto's film method using fresh and unfixed samples (Kawamoto, 2003). Briefly, fish at 3 months were anesthetized and then cut into three pieces. The cut samples were embedded into embedding medium before being soaked in cooled isopentane with liquid nitrogen. Using cryofilm tape, samples were sectioned at 20 μm thickness. Sections were fixed with 4% PFA for 5 min then washed three times using PBS. Takara TRACP and ALP double-stain Kit was used for the detection of alkaline phosphatase according to manufacture. Staining was performed at room temperature for 30 min.

2.7 RNA extraction and cDNA synthesis

To perform relative mRNA expression analysis, total RNA was extracted from vertebral bone using RNeasy Lipid tissue mini kit (QIAGEN) according to the manufacturer′s protocol. Subsequently, RNA concentration was measured using Q5000 micro-volume spectrophotometer (TOMY). About 500 ng of extracted RNA was used for cDNA synthesized using ReverTra Ace qPCR RT kit following the manufacturer′s protocol. The cDNA was stored at −20 ^{O}C until use.

2.8 Cell-attached patch clamp mode

To confirm whether the 11 amino acid deletion affects Piezo1 channel function, we performed patch-clamp experiment using cell-attached mode. The cDNAs of zebrafish wildtype-*piezo1* and 11-amino acids deletion mutant were cloned into pIRES2-GFP vector, respectively. The constructed plasmids then were purified using nucleospin plasmid-transfection grade (TAKARA) and transfected into piezo1-deficient N2A cells (Sugisawa et al., 2020). About 48–72 h after transfection, the channel activities were recorded.

Briefly, the recordings were conducted at room temperature with a mean pipette resistance of 4.0–6.0 MΩ. In this recording, the pipette solution contained 140 mM NaCl, 5 mM KCl, 2 mM $MgCl_2$, 2 mM $CaCl_2$, 10 mM hepes (pH 7.4 adjusted with NaOH), and 10 mM glucose same with bath solution. Following giga-seal formation, the holding potential was clamped to −80 mV and the channel was stimulated by applying a negative pressure of −40 mmHg.

2.9 qPCR

The primers for this experiment are listed in Supplementary Table S3. To perform qPCR analysis, SYBR Green PCR Master Mix (Applied Biosystem) was used and carried out in the Applied Biosystems™ StepOne™ Real-Time PCR System. The amplification conditions were 95°C for 10 min, 40 cycles at 95°C for 15 s, and 60°C for 1 min. All reactions were performed in triplicate. Relative mRNA expressions were normalized to *beta-actin* (*actb1*) gene. Primer sets for qPCR were listed in Supplementary Table S3.

2.10 Rescue experiment with introducing functional *piezo1*

Zebrafish *piezo1* coding sequence (CDS) was amplified by PCR and then cloned into the pTol2 plasmid with *osterix* promoter (Kawakami et al., 2000; Renn and Winkler, 2009). Sequences of the primers used to amplify *piezo1* CDS are piezo1-F1_Sal1; 5-TTT TGGCAAAGAATTGTCGACCACCATGGAGCTTCAGGTGGT A-3′ and piezo1-R1_Not1; 5′-CGTTAGGGGGGGGGGCGGCC GCTCAGTTGTGATTCTTCTCTC-3′. In addition, since Piezo1 protein has many hydrophobic domains that cause toxicity in *E. coli*, intron 10 and intron 42 were inserted in CDS. Purified plasmid

was mixed with *in vitro* synthesized Tol2 Transposase mRNA (10 ng/μL each), and the mixture was injected into fertilized eggs (1 nL/egg) at the single-cell stage.

2.11 Statistical analysis

All data are presented as mean ± SD. Statistical analysis was performed by two-tailed Student's t-test for the two groups and by one-way analysis of variance (ANOVA) test and Tukey's post-test for the three groups. Differences were considered statistically significant at $p < 0.05$.

3 Result

3.1 Generation of piezo null mutant

Zebrafish have three different *piezo* genes: *piezo1* (XM_691263), *piezo2a* (XM_021470255), and *piezo2b* (XM_021468270). In whole-mount *in situ* hybridization using 48hpf larval zebrafish, both expressions of *piezo1* and *piezo2a* were detected in many tissues, including bone, while *piezo2b* expression was limited to cells of the nervous system (Faucherre et al., 2013). This suggests that zebrafish *piezo1* and *piezo2a* may have redundant functions.

To generate *piezo* activity-deficient zebrafish, we utilized the CRISPR/Cas9 method (Ran et al., 2013). A guide RNA targeting the internal sequence of exon 5 of *piezo1* gene or exon 4 of *piezo2a* gene was synthesized and co-injected with Cas9 protein into one-cell stage wildtype embryos. Following the screening of several founders that transmitted to the F1 progeny, we established two independent stable lines of each mutant gene. We verified the sequence of each mutant allele and confirmed that each mutant gene generated a premature termination codon (PTC) as a result of an altered mRNA reading frame (Supplementary Figures S1A–D).

We assessed the relative mRNA levels of *piezo1* and *piezo2a* in each homozygous mutant, but observed no significant changes in expression. This suggests that the Non-mediated mRNA decay (NMD) pathway may not have occurred (Supplementary Figures S1E, F).

3.2 Phenotypes of the zebrafish with double mutations of *piezo1* and *piezo2a*

As we expected from the similarity of expression pattern, the single mutants of $piezo1^{-/-}$ and $piezo2a^{-/-}$ were viable and fertile. Neither mutant showed morphological abnormalities in the larval and juvenile stages (Supplementary Figure S2).

Next, to obtain large numbers of fish with double mutations, fish sharing the $piezo1^{-/+}$; $piezo2a^{-/-}$ genotype were crossed. In this case, 2%–30% of the individuals died around 10 days after fertilization. When the gene was examined, fish with the double homozygous mutation survived to day 8, but all died by day 11 (Supplementary Figure S3A). This indicates that the double mutant fish is lethal in the juvenile stage.

The surviving fish on day 8 showed a shortening of body length (Supplementary Figure S3B) and curvature of the body axis (Figures 1A, B). In addition, the swim bladder was not fully inflated (90%) (Figure 1B arrowhead). Alizarin red S staining revealed that all double homozygous mutants showed inadequate bone formation such as small vertebral segment, hemivertebral and vertebral bone missing compared to their siblings (Figures 1C–F). From these data, it is shown that Piezo channels are essential for bone formation and mineral deposition during early development. However, because of the lethality in the young stage, it is not suitable for pathological model of scoliosis.

3.3 Mosaic mutant displays bone curvature

If the cause of death is an abnormality that occurs in an organ other than the spine, CRISPRants (F0 mutants), in which loss of function of the target gene occurs in a mosaic fashion, may avoid the lethality that occurs early in development and allow us to study effects during later developmental stages (She et al., 2019; Buglo et al., 2020). To test this possibility, we injected sgRNAs targeting *piezo1* or *piezo2a* into one-cell stage embryos in a *piezo2a* null mutant or *piezo1* null mutant background (Figure 1G).

As a result, no abnormal phenotypes were observed in either mutant background at the larval to juvenile stage. However, by 17 days post-fertilization (dpf), a small kink of the spine near the tail of the body occurred. This curvature was even more severe in adulthood in more than 80% of $piezo2a^{-/-}$ injected with *piezo1* sgRNA and about 50% of $piezo1^{-/-}$ injected with *piezo2a* sgRNA, with the abnormal vertebrae located near the distal end of the tail and near the hypural complex (Figures 1H–J; Supplementary Figure S4).

In this mosaic mutants, the irregular bone morphology shares some similarities with scoliosis, particularly in its occurrence during the process of growth. This fact suggests that artificial mutations in the *piezo* genes may be able to create a pathological model of scoliosis, but in order to create a useable model, lethality must be avoided by simpler methods.

3.4 Generation of *piezo1* in-frame mutant

Next, we analyzed in-frame mutation of the *piezo1* gene. In the process of creating a deletion mutation in the *piezo1* gene, an in-frame mutation was obtained when a guide RNA targeting the splice acceptor sequence in exon 2 was used. In this allele, the removal of the splice acceptor site "AG" resulted in a deletion of 11 amino acids, without the insertion of a premature stop codon (Figures 2A, B). The mutant was designated as $piezo1^{11aa\ del/11aa\ del}$ and the resulting protein was named 11aa del-Piezo1. The 11 amino acid deletion region is conserved among vertebrates (Supplementary Figure S5) and likely plays an important role in Piezo1 channel function.

First, we measured mRNA levels of 11aa del-Piezo1 using qPCR to determine whether *piezo1* gene in $piezo1^{11aa\ del/11aa\ del}$ is transcribed normally. The results showed that the mRNA level of *piezo1* in $piezo1^{11aa\ del/11aa\ del}$ mutant was reduced by almost half compared to the wildtype (Figure 2C), while there was not a significant difference in *piezo2a* mRNA level (Figure 2D).

Next, we assessed the channel activity of 11aa del-Piezo1 using a cell-attached patch clamp assay. The zebrafish *piezo1* genes were obtained from both the wildtype and mutant forms, inserted into an expression

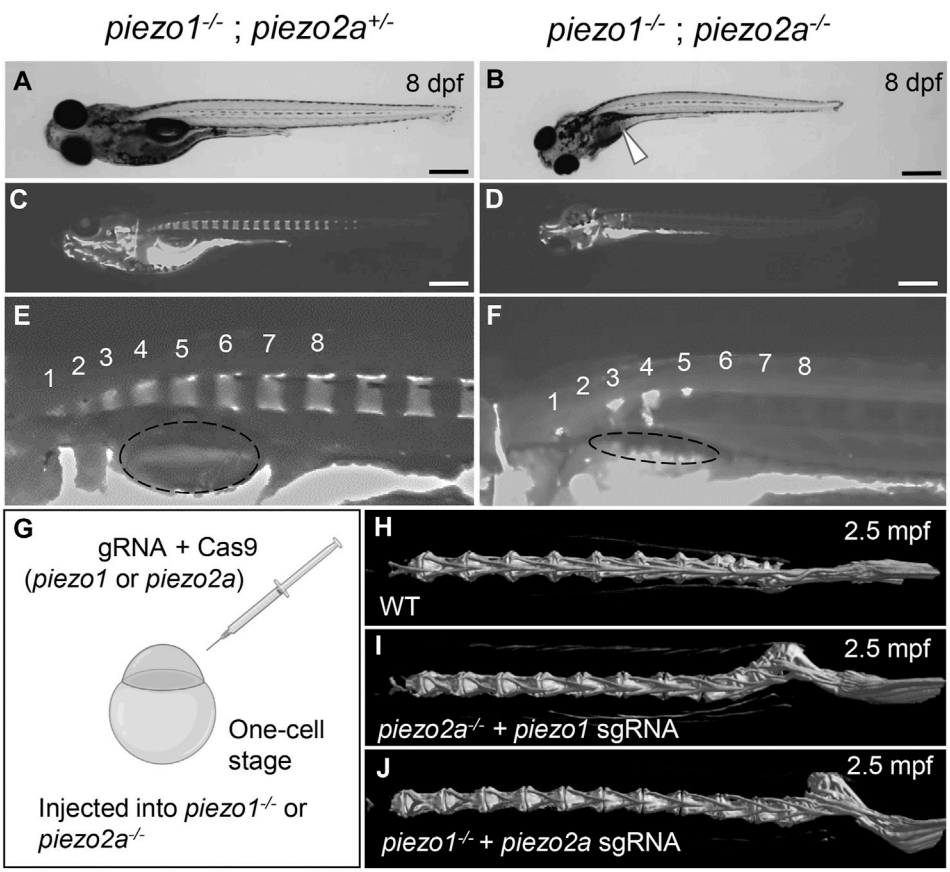

FIGURE 1
piezo1 and *piezo2a* are essential for bone formation and mineral deposition in early stage of development. **(A,B)** Gross phenotypes and **(C,D)** mineralization patterns of sibling and *piezo1*$^{-/-}$; *piezo2a*$^{-/-}$ mutant at 8 days after fertilization (dpf). White arrow indicates uninflated swim bladder. Scale = 500 μm. **(E,F)** Magnified images of the anterior body of sibling and double mutant. Numbers 1 to 8 indicate the position of each vertebral bone. The dashed circle indicates swim bladder. Notably, the swim bladder in double mutant was small and uninflated. **(G)** Schematic diagram of generating piezo transient KO mutant (CRISPRant). Comparison of 3D reconstruction of micro-CT images of vertebral bone at caudal part from **(H)** wildtype, **(I)** *piezo1* sgRNA injected to *piezo2a*$^{-/-}$, and **(J)** *piezo2a* sgRNA injected to *piezo1*$^{-/-}$ at 2.5 months after fertilization.

vector, and transfected into *piezo1*-deficient N2A cells. After about 48 h of incubation, channel activity was recorded. It was found that in wildtype Piezo1, an inward current flowed when negative pressure was applied with a pipette, whereas only a very weak current flow was observed in the 11aa del-Piezo1 (Figures 2E, F). These results indicated that the deletion of 11 amino acids in the N-terminal domain of Piezo1 caused a functional defect in the Piezo1 channel. In the following experiments, we examine the effects of this on spine formation in detail.

3.5 *piezo1* in-frame mutant (*piezo1*$^{11aa\ del/11aa\ del}$) develops juvenile-onset scoliosis

At 4 dpf, there were no critical differences between wildtype and *piezo1*$^{11aa\ del/11aa\ del}$. However, at later stages, during the larval and early juvenile period, the body length of the mutant fish became relatively shorter than that of wildtype, suggesting the late-onset abnormality in the vertebrae (Figure 3B).

Alizarin red staining to track vertebral formation at 8 dpf, 20 dpf, and 35 dpf showed that the spines gradually curved as the fish grew, and heterotopic bone formation was occurring in the intervertebral space. Unlike double mutant fish, however, there was no significant variation in the number or spacing of vertebrae or in the morphology of individual vertebrae (Figure 3A).

In adults, the curvature of the spine was even more severe, and it appears to be folded in particularly severe areas. This curvature occurs both laterally and vertically (Figure 3A). In general, these symptoms resemble human scoliosis (Cheng et al., 2015). Although sexual dimorphism is one of idiopathic scoliosis features in human, which has also reported in several zebrafish scoliosis mutant model (Hayes et al., 2014; Marie-Hardy et al., 2021), there was no sex bias in *piezo1*$^{11aa\ del/11aa\ del}$ mutant fish. Both sexes developed similar severity of curve penetrance (Figure 3C, Supplementary Figure S6).

3.6 Detailed observation of vertebra shape by micro-CT

Next, micro-CT measurements were taken to examine the shape of the individual vertebrae and surrounding bone (Figures 4A, B). As shown in Figure 3A, the vertebrae were generally curved, but there were no significant changes in the shape of the neural or haemal

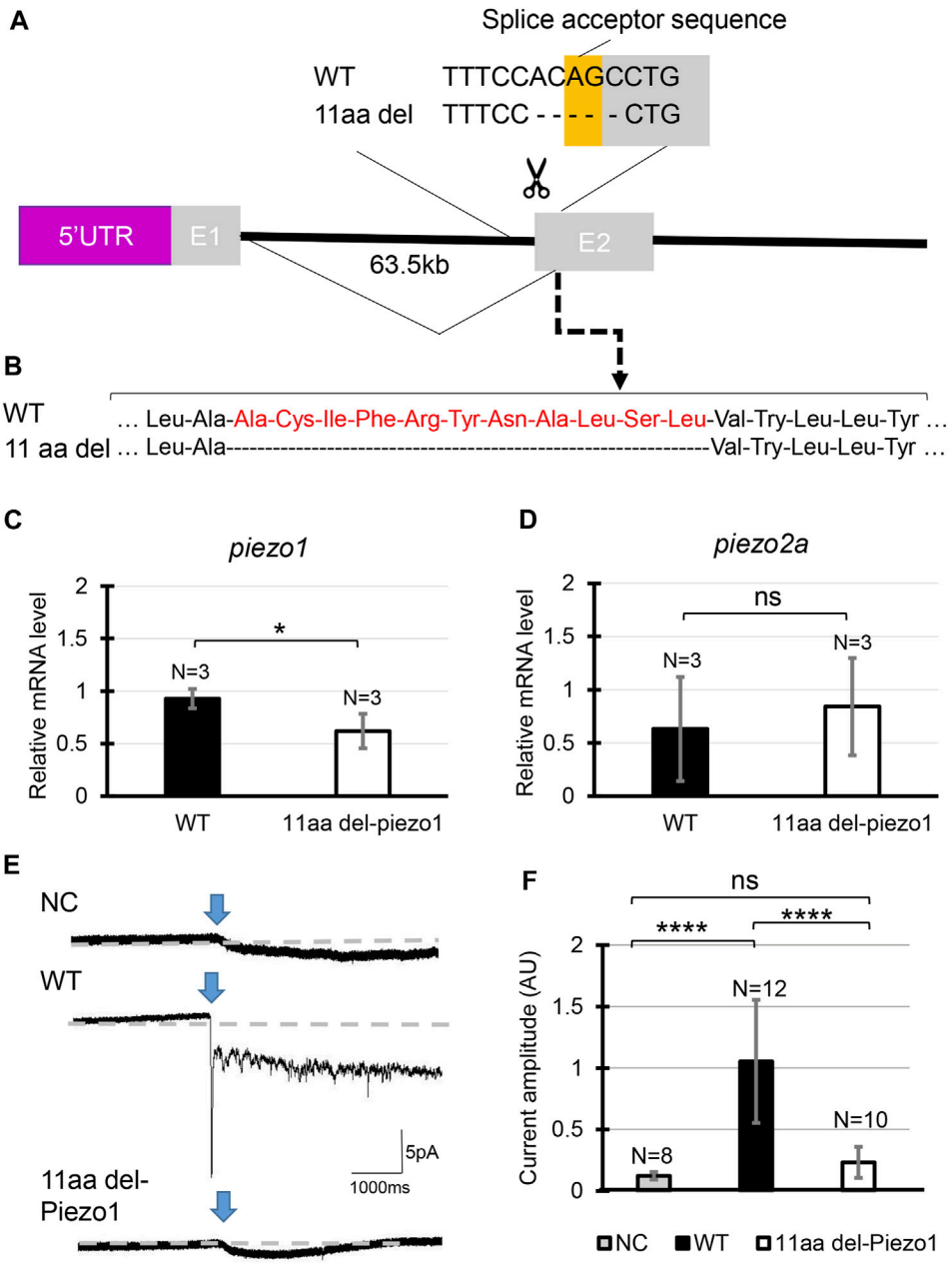

FIGURE 2
Generating *piezo1* in-frame mutant. **(A)** Schematic illustration of CRISPR target in *piezo1* gene with a guide RNA targeting splice acceptor site of exon2. Through this guideRNA, the splice acceptor site was eliminated, generating cryptic acceptor site which deleted several bases of internal exon 2. **(B)** Confirmation of amino acid sequence. Quantification of relative mRNA level of **(C)** *piezo1* and **(D)** *piezo2a* in $piezo1^{11aa\ del/11aa\ del}$. Values are presented as mean ± SD and analyzed using Student's t-test. $^{**}p < 0.01$. **(E)** Representative traces of negative pressure-induced inward currents recorded at −80 mV in negative control (NC), zebrafish Piezo1 Wildtype (WT), and zebrafish 11aa del-Piezo1. Blue arrows indicate the time when negative pressure was applied. Grey dashed lines indicate baseline of the current. **(F)** Measurement of current amplitude, measured in arbitrary units (AU). Values are presented as mean ± SD and analyzed using one-way ANOVA followed by Tukey's test. $^{****}p < 0.0001$. ns indicates not significant.

arches. To assess the deformity of individual vertebrae causing the curvature, the size of individual vertebrae was measured and expressed as the ratio of anterior/posterior height (H1/H2) and dorsal/ventral length (L1/L2) (Bearce et al., 2022). Figure 4 shows data for the 8th to 13th vertebrae of 5 individual fish. In the wildtype, both ratios were approximately 1, with very little variation among individuals or by vertebral position (Figure 4C). In the mutant, however, there was variation for each vertebra, and the variation in length ratio (L1/L2) was considerably greater than the variation in height ratio (H1/H2) (Figure 4D). This fact suggests that the curvature of the spinal column has caused more longitudinal compression, which is also characteristic of scoliosis in humans (Shea et al., 2004; Schlager et al., 2018).

We assessed Tissue Mineral Density (TMD) using CT data to evaluate calcium deposition in bones. In general, wildtype fish exhibited high TMD (Figure 4E). In the case of $piezo1^{11aa\ \ del/11aa}$

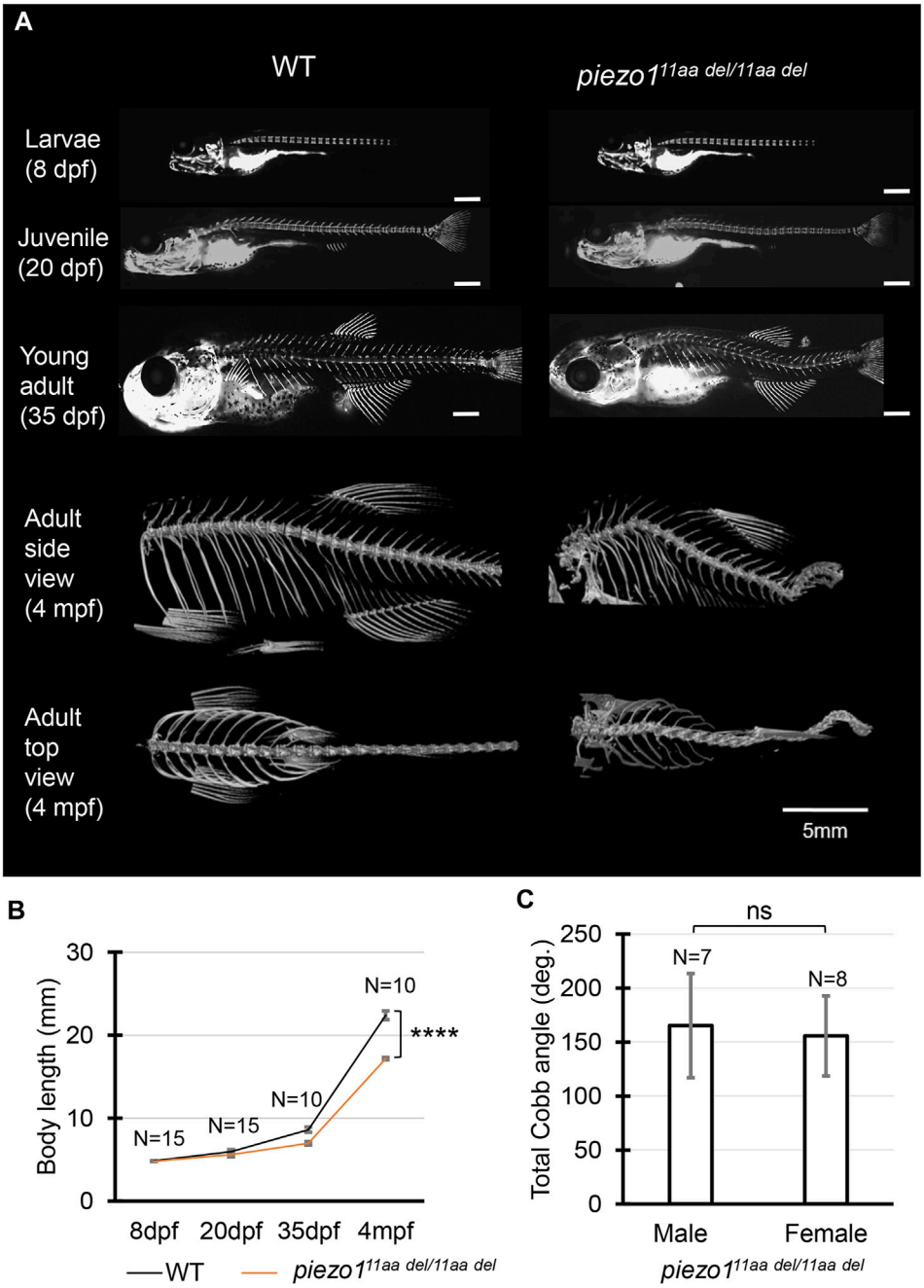

FIGURE 3
Phenotype of *piezo1* in-frame mutant (*piezo1*$^{11aa\ del/11aa\ del}$). **(A)** Time course observation of mineralized bone using alizarin red S staining between wildtype and *piezo1*$^{11aa\ del/11aa\ del}$ mutant from larvae (8 dpf) to young adult (35 dpf) (Used scale 500 μm) and 3D rendering of micro-CT images of wildtype and *piezo1*$^{11aa\ del/11aa\ del}$ mutant at 4 months. **(B)** Graph depicting body length. **(C)** Average of total Cobb angle. Cobb angles were measured according to previous study (Bearce et al., 2022). Values are presented as mean ± SD and analyzed using Student's t-test. *****p* < 0.0001*. ns means non-significant.

^{del}, the curved bones exhibited elevated TMD, likely attributable to increased mechanical stress from bone compression (Bagwell et al., 2020). To mitigate measurement bias arising from bone irregularities, we specifically measured TMD in the non-curved bones, particularly focusing on the central portion of the hourglass-shaped bone. We found that *piezo1*$^{11aa\ \ del/11aa\ \ del}$ at 3 months of age had predominantly lower TMD values than the wildtype (Figures 4E, F). This is consistent with various reports when they assessed the bone mineral density in scoliotic patients (Sarioglu et al., 2019; Li et al., 2020; Almomen et al., 2021).

3.7 Abnormal osteoblast function

Due to the decreased TMD value observed in the mutated bones, we opted to examine the bone metabolism profile. In individuals

10.3389/fgene.2023.1321379

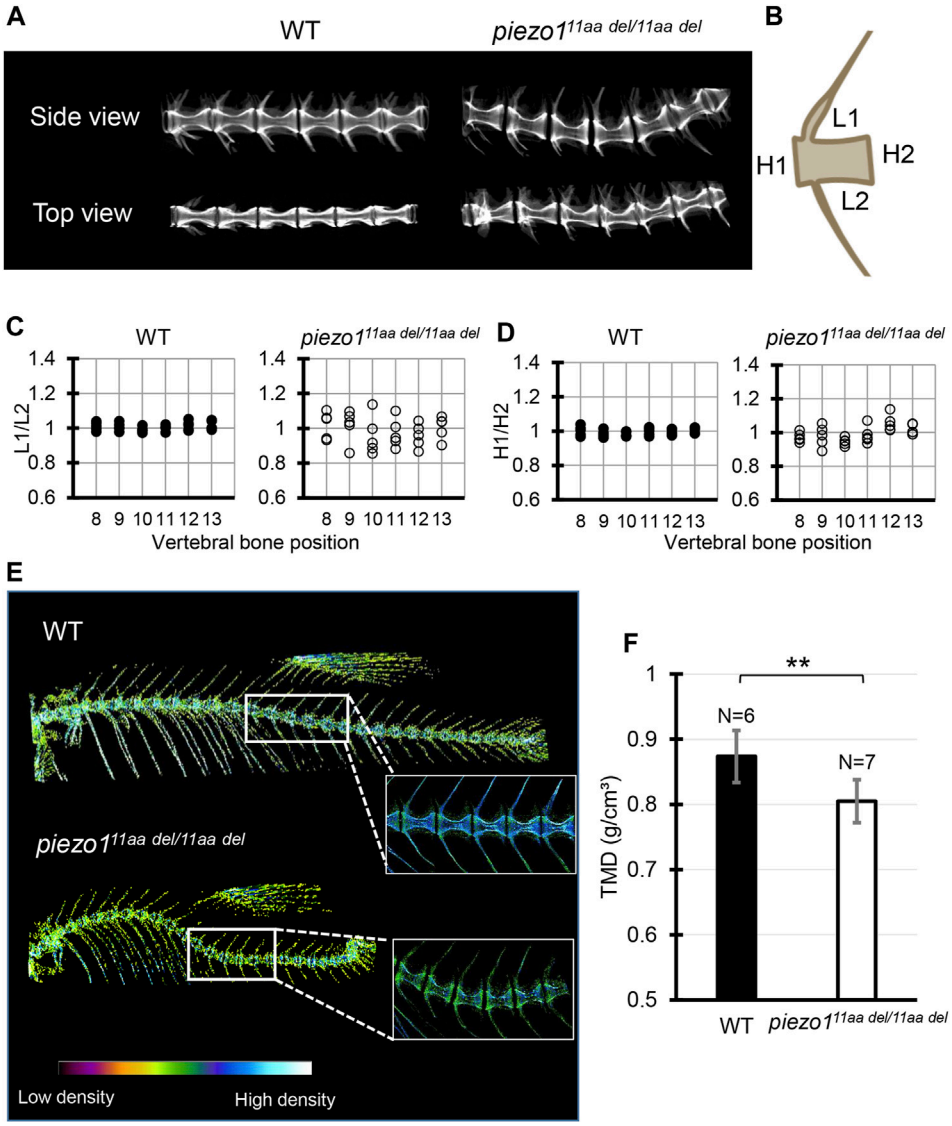

FIGURE 4
Detailed analysis of vertebra shape. **(A)** Comparison of 3D reconstruction of micro-CT images of vertebral bone between wildtype and *piezo1*$^{11aa\ del/11aa\ del}$ at the abdominal part from side and top view. **(B)** Schematic diagram and quantification of the **(C)** length ratio (L1/L2) and **(D)** height ratio (H1/H2) of single vertebrae measurement. About 6 vertebrae from wildtype (N = 5) and mutant (N = 5) were assessed. Length aspect ratio and height aspect ratio were significantly more variable in mutant ($p < 0.0001$, analyzed using F-test two samples for variances). **(E)** The micro-CT reconstructions of 3 months zebrafish from both the wildtype and *piezo1*$^{11aa\ del/11aa\ del}$ mutant specimens were performed. The reconstructions were color-enhanced to represent bone density value. To minimize measurement error, trunk or abdominal part was chosen to measure TMD value due to low bone kinks, indicated as white boxes. **(F)** Measurement of Tissue Mineral Density (TMD). Values are presented as mean ± SD and analyzed using Student's t-test. $^{**}p < 0.01$.

with osteoporosis, diminished bone density is consistently linked to reduced osteoblast activity or heightened osteoclast activity (Guido et al., 2009). Since previous study has verified the *piezo1* gene expression is higher in osteoblast than osteoclast, we mainly analyzed osteoblast activity using alkaline phosphatase staining (Sun et al., 2019).

Alkaline phosphatase (ALP) is not exclusively produced from bone, but also from liver, kidney, small intestine, and so on. To avoid false observation, fixed region of interest (ROI) was put around growth plate region indicating bone alkaline phosphatase. As shown in Figures 5A, B, wildtype fish displayed larger alkaline phosphatase positive area than *piezo1*$^{11aa\ del/11aa\ del}$. Low levels of alkaline phosphatase in scoliotic mutant fish indicate reduced bone formation, as ALP is produced as a byproduct of osteoblast activity.

Furthermore, we generated transgenic fish expressing green fluorescence protein (GFP) in *Osterix* promoter, an osteoblast-specific promoter (Iwasaki et al., 2018). Since GFP-positive osteoblasts are observable in transgenic (*osx-GFP*) larvae, the progression of osteoblast differentiation and the formation of bone can be directly tracked. The stable transgenic fish (*osx-GFP*) were crossed twice with *piezo1*$^{11aa\ del/+}$ to generate wildtype;(*osx-GFP*) and *piezo1*$^{11aa\ del/11aa\ del}$; (*osx-GFP*) siblings. As expected, *piezo1*$^{11aa\ del/11aa\ del}$ mutant fish exhibited lower GFP signal than wildtype siblings (Figures 5C, D). This suggests that not only

10.3389/fgene.2023.1321379

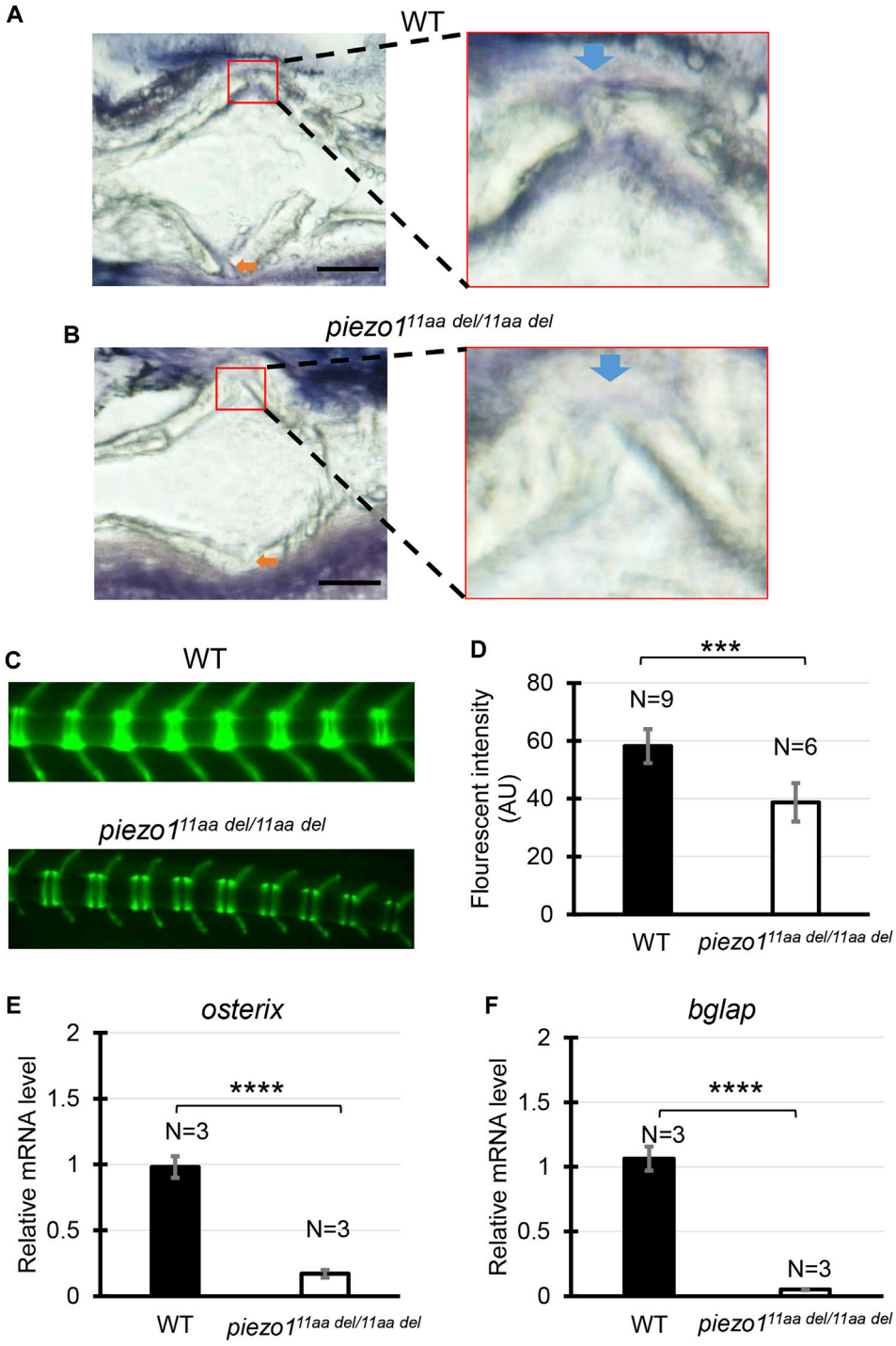

FIGURE 5
Abnormal osteoblast function. **(A,B)** Representative image of alkaline phosphatase staining in vertebral bone section of wildtype (N = 4) and *piezo1*$^{11aa\ del/11aa\ del}$ (N = 5). Red boxes indicate the magnified area of growth plate. Blue arrow indicates center of growth plate, orange arrow indicates growth plate at the opposite site. Scale bar is 100 μm. **(C)** Fluorescence images of vertebral bone of wildtype; (*osx-GFP*) and *piezo1*$^{11aa\ del/11aa\ del}$; (*osx-GFP*) at 25 dpf. **(D)** Quantitative analysis of fluorescence area. Values are presented as mean ± SD and analyzed using Student's t-test. ***$p < 0.001$. *mRNA level of* **(E)** osterix, *mid-stage osteoblast marker gene, and* **(F)** osteoclacin/bglap, *late-stage osteoblast marker gene.* Values are presented as mean ± SD and analyzed using Student's t-test. ****$p < 0.0001$.

osteoblast activity is reduced but osteoblast differentiation is also affected in this scoliotic mutant fish.

To further confirm these results, we measured two osteoblast marker genes, *osterix* and *bglap/osteocalcin* by quantitative PCR analysis. As shown in Figures 5E, F, *piezo1*$^{11aa\ del/11aa\ del}$ mutant fish showed a significant reduction in the expression of osteoblast-specific genes. Together, these data confirm that *piezo1*$^{11aa\ del/11aa\ del}$ mutant fish showed low osteogenesis.

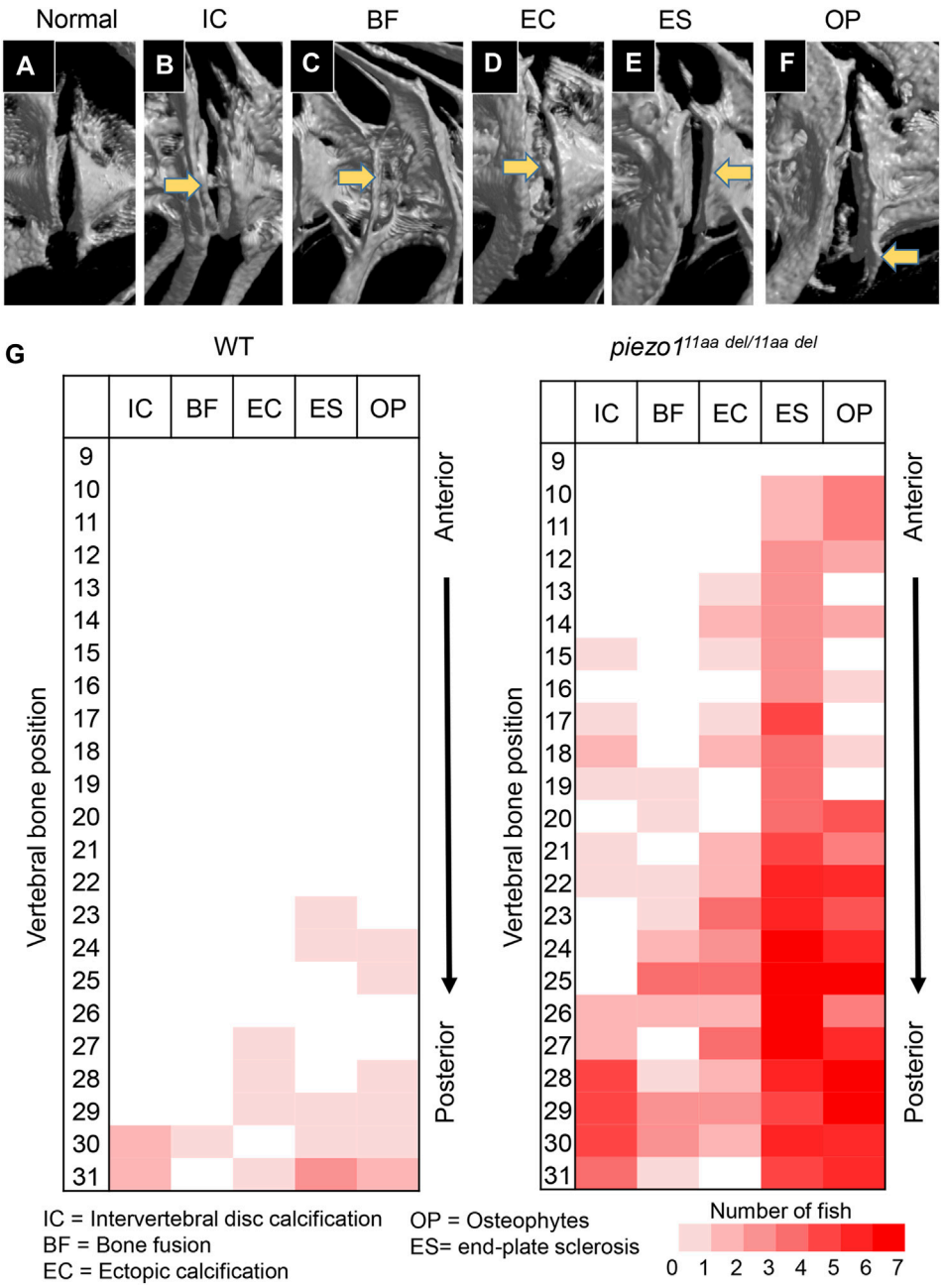

FIGURE 6
Abnormal changes of vertebral bone in *piezo1*$^{11aa\ del/11aa\ del}$. **(A)** Normal feature of bone; **(B)** Intervertebral disc calcification (IC); **(C)** Bone fusion (BF); **(D)** Ectopic calcification (EC); **(E)** End-plate sclerosis (ES); **(F)** Osteophytes formation (OP). **(G)** Heat map depicting the position and frequency of abnormal features of bone between wildtype and *piezo1*$^{11aa\ del/11aa\ del}$.

3.8 Progressive abnormalities in vertebral column of *piezo1*$^{11aa\ del/11aa\ del}$

Several studies have shown that adolescent idiopathic scoliosis can lead to intervertebral disc (IVD) degeneration in later life (Bertram et al., 2006; Hristova et al., 2011; Akazawa et al., 2017). Many of the abnormal bone features described, such as osteophyte formation, endplate sclerosis, facet joint changes, IVD narrowing, and ectopic calcification, have been observed in individuals with intervertebral disc degeneration. To discern irregular bone alterations in the spine, a comparison was made between 3D-rendered micro-CT images of wildtype and mutant fish. Subsequently, an assessment was conducted to determine the frequency of abnormal bone characteristics observed in the spine. From this analysis, there were at least five abnormal bone features in *piezo1*$^{11aa\ del/11aa\ del}$ mutant fish at the age of 5 months, encompassing IVD calcification (IC), bone fusion (BF), ectopic bone calcification (EC), end-plate sclerosis (ES), and osteophytes (OP) (Figures 6A–F) (Kague et al., 2021).

As shown in Figure 6G, although had similar ages, bone abnormalities were more frequent in mutant than wildtype. This

10.3389/fgene.2023.1321379

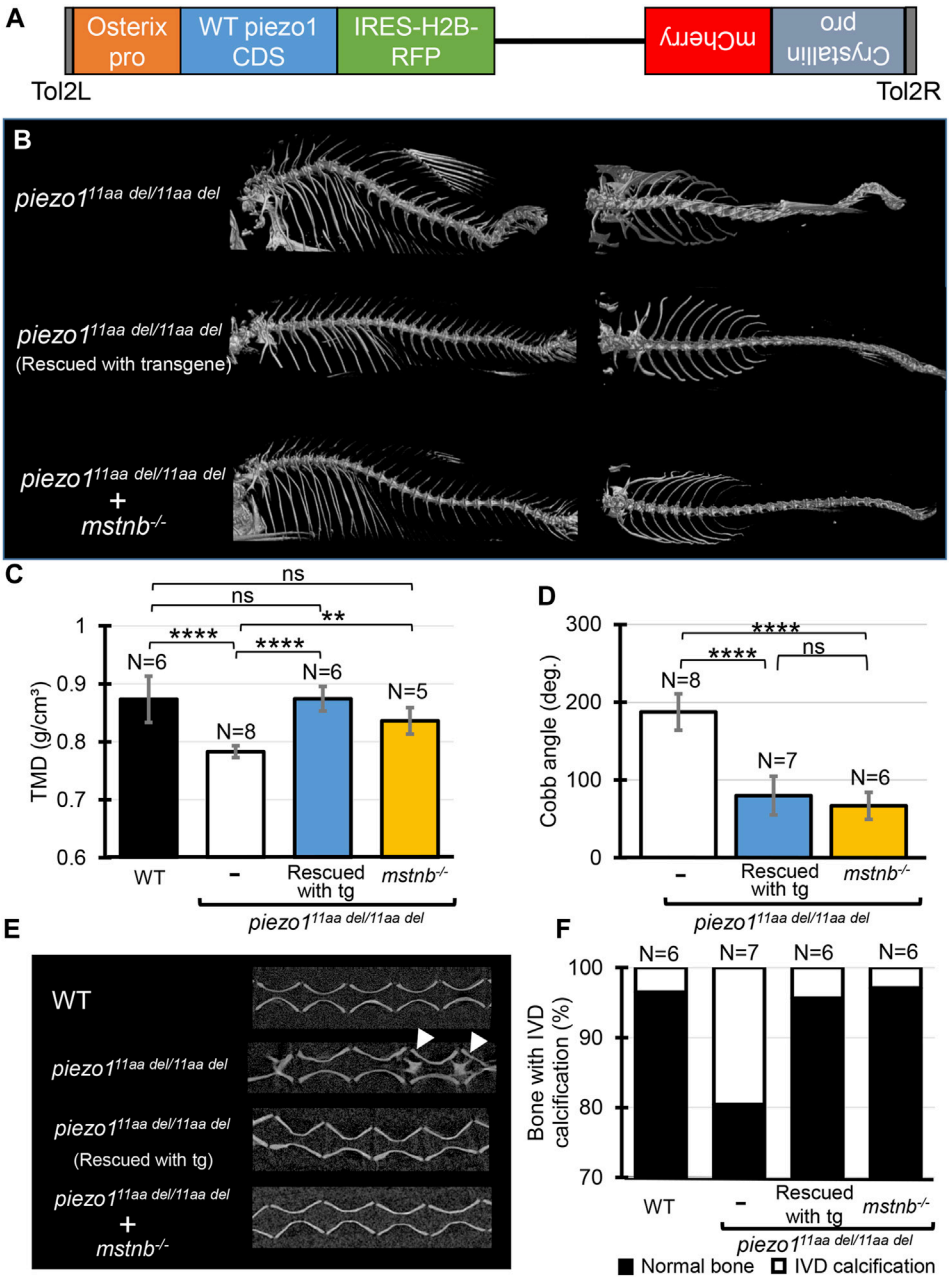

FIGURE 7
Introducing functional *piezo1* gene or increasing muscle mass can alleviate scoliosis symptoms. **(A)** Schematic diagram of rescue plasmid. Notably, *sp7/osterix* promoter was used to express functional *piezo1* gene. **(B)** Comparison of 3D reconstruction of micro-CT images. **(C)** Quantification of TMD from 5 individual segments of abdominal vertebrae of wildtype (N = 6), *piezo1*$^{11aa\ del/11aa\ del}$ mutant (N = 8), rescue mutant fish (N = 6), and double mutant of *piezo1*$^{11aa\ del/11aa\ del}$; *mstnb*$^{-/-}$(N = 5). **(D)** Combined Cobb angle of *piezo1*$^{11aa\ del/11aa\ del}$ mutant (N = 8) rescue mutant fish (N = 7), and double mutant of *piezo1*$^{11aa\ del/11aa\ del}$; *mstnb*$^{-/-}$ (N = 6). **(E)** Sagittal section of the spine. Rescue mutant and *piezo1*$^{11aa\ del/11aa\ del}$; *mstnb*$^{-/-}$ have reduced the number of bone with IVD calcification (white arrows). **(F)** Graph depicting the percentage of bone with IVD calcification across bone segments 9 to 31. Values are presented as mean ± SD and analyzed using one-way ANOVA followed by Tukey's test. ns = non-significant; $^{**}p < 0.01$; $^{***}p < 0.001$; $^{****}p < 0.0001$.

suggests *piezo1*$^{11aa\ del/11aa\ del}$ mutant fish might have premature bone degeneration. Malformation of vertebrae can occur at any site, regardless of the type of morphological abnormality, but are more frequent at sites close to the tail. Particularly distinct are the intervertebral calcification sites, with more than 80% occurring in the 28th to 30th vertebrae, where the physical stress from tail movement is expected to be greatest. This suggests that the cause of these bone abnormalities is mechanical stress.

3.9 Introducing functional *piezo1* gene into *piezo1* scoliosis mutant could develop normal spine

Identification of the causative cell is important for use as a disease model. The most likely candidate is osteoblasts, but since the *piezo1* gene is expressed in many tissues, we cannot rule out osteoblasts as the cause of the mutation in *piezo1*$^{11aa\ del/11aa\ del}$

mutant. Therefore, we attempted to express *piezo1* using the osteoblast-specific promoter *sp7/osterix* to see if the mutation could be rescued (Figure 7A).

Results are shown in Figure 7B, as expected, the mutant fish harboring transgene with the rescue plasmid showed a nearly normal phenotype (Supplementary Figure S7). Although some small bones were slightly bent along the vertebrae, the reduced phenotype in the rescue mutant was confirmed in all of the TMD, Cobb angle, and percentage of bone with IVD calcifications (Figures 7C–F).

This result confirms that the cells responsible for the bone morphological abnormalities in *piezo1* are osteoblasts. Furthermore, it shows that the severity of the morphological abnormality can be regulated by artificially altering the expression level of *piezo1*. This will increase the utility of the *piezo1*$^{11aa\ del/11aa\ del}$ fish as a pathological model.

3.10 Increase muscle mass could alleviate scoliosis symptoms

To evaluate the utility of *piezo1*$^{11aa\ del/11aa\ del}$ mutant fish as a model for pathology, it is necessary to determine whether the abnormal bone morphology of fish responds in the same manner as in humans to manipulations that aggravate or alleviate the symptoms of scoliosis. Scoliosis that develops during adolescence can sometimes be attributed to muscle defects (Lv et al., 2021). Furthermore, exercise, especially weight-bearing exercises that increase muscle mass, has been shown to be an effective treatment for scoliosis (Lau et al., 2021; Hui et al., 2022). Based on these facts, we hypothesized that increasing muscle mass might reduce scoliosis-like symptoms in *piezo1*$^{11aa\ del/11aa\ del}$ mutant fish. In fish and mice, inhibition of the *myostatin (mstnb)* gene, a protein that regulates muscle development (Welle et al., 2007; Suh et al., 2020) can increase muscle mass with little effect on other organs. Therefore, disrupting the *myostatin* gene in *piezo1*$^{11aa\ del/11aa\ del}$ fish can easily be used to study the relationship between muscle mass and the pathological level of scoliosis.

Using previously published guide RNA (Gao et al., 2016), zebrafish *myostatin* knockouts were produced by CRISPR/Cas9. Zebrafish *mstnb*$^{-/-}$ exhibited relatively larger body size compared to wildtype (Gao et al., 2016), with a clear increase in muscle mass around the spine (Supplementary Figure S8). Next, *myostatin* knockout zebrafish were crossed twice with *piezo1*$^{11aa\ del/+}$ to examine the relationship between increased muscle mass and scoliosis severity. Figure 7 shows an overview of the vertebrae and the statistical data. As expected, the strength of the spinal curvature decreased with increasing muscle (Figure 7B), and tissue mineral density increased (Figure 7C). When quantified in terms of Cobb angle, it decreased to almost 30% (Figure 7D). Also, abnormal calcification in the intervertebral disc (IVD) region was also barely observed (Figures 7E, F). This suggests a decrease in bone degeneration. These findings are strong evidence that increasing muscle mass alleviates scoliosis and promotes bone formation, suggesting a potential therapeutic approach for the treatment of scoliosis. *piezo1*$^{11aa\ del/11aa\ del}$ fish may be used effectively as a pathological model for scoliosis. We suggest that *piezo1*$^{11aa\ del/11aa\ del}$ fish is a good model for the treatment of scoliosis, as they have been shown to be able to increase the muscle mass of the spine and to increase the bone mineral density of the spine.

4 Discussion

Scoliosis is a disease caused by the almost unique posture of humans in the vertebrate world, in which they stand upright on two legs, and it has been difficult to obtain an experimental system that can serve as a model for the disease (Castelein et al., 2005; Bobyn et al., 2015; Xie et al., 2022). On the other hand, there have been cases of scoliosis-like symptoms in fish (Gorman et al., 2007; Gorman and Breden, 2009), and it is thought that the longitudinal compression of the spine caused by the propulsive force of the caudal fin is similar to that caused by the upright posture in humans. We have established a pathological model of scoliosis in zebrafish by manipulating the *piezo* genes, which are mechanotropic stimulus receptors in the cells. Zebrafish have two *piezo* genes (*piezo1* and *piezo2a*) involved in bone formation. When both genes were knocked out, various abnormalities including bone formation appeared in early development and early death occurred. However, an in-frame mutation in the *piezo1* gene (11 amino acid deletion) was not lethal and caused morphological abnormalities of the spine similar to scoliosis in humans. The fact that the morphological abnormalities occur later in life and that bone density is reduced, also suggests that the zebrafish spinal morphology may be homologous to human scoliosis. Since zebrafish can be easily bred in large numbers and genetic manipulation tools have been developed, it is expected that mutant zebrafish will be used to study the pathogenesis of scoliosis and to screen for therapeutic agents.

4.1 Usefulness as a pathological model

The pathological model of scoliosis created in this study using zebrafish has several advantages besides the ease of rearing a large number of animals. As shown in Figure 7, the severity of the disease can be modulated by the expression of normal *piezo1* and *piezo2a* genes. This could be a useful property when screening for therapies. When screening for therapeutic agents, it is expected that if the severity of the model is too strong, the effect will not be apparent, and if the severity is too weak, the data may be unstable. Screening for individuals of varying severity would reduce the likelihood of missing an effective drug. Another advantage is the ability to test the efficacy of treatments other than relaxing agents, such as physical therapy, as in the present study, where muscle augmentation due to deletion of the *myostatin* gene induced a resolution of symptoms. A more advanced approach would be to investigate the relationship between exercise therapy and scoliosis, such as artificially inducing muscle contraction with light.

4.2 Causal relationship between scoliosis and osteoporosis

Although scoliosis and osteoporosis are distinct skeletal conditions with separate sets of symptoms and underlying causes, there is a suggested connection between them. Numerous clinical

reports have indicated that individuals with idiopathic scoliosis often exhibit lower bone mineral density (BMD) (Li et al., 2008; Sadat-Ali et al., 2008; Nishida et al., 2023; Wu et al., 2023), a key indicator of osteoporosis. Similar to these studies, we also reported remarkably lower BMD values in *piezo1*$^{11aa\ del/11aa\ del}$ mutant compared to siblings. However, it remains unclear whether osteoporosis plays a causative role or is a consequence of scoliosis.

Based on current knowledge, it is plausible that osteoporosis may be an underlying factor contributing to the development of scoliosis. Histological examinations of trabecular bone in idiopathic scoliosis patients have shown decreased osteoblast activity (Cheng et al., 2001). Additionally, children diagnosed with idiopathic scoliosis have demonstrated diminished osteogenic differentiation potential in their mesenchymal stem cells (Park et al., 2009; Chen et al., 2016). These findings suggest that the decline in osteoblast activity, leading to a reduction in BMD, may occur prior to the formation of lateral spinal curvature. Low bone density resulting from abnormal osteogenic activity could increase the risk of bone fractures. The presence of microfractures may, in turn, contribute to bone asymmetry, potentially exacerbated by axial loading. Eventually, this leads to the development of spinal deformity in a cyclical and interdependent manner.

4.3 *piezo1* and *piezo2a* might have overlapping function

In our first finding, we demonstrated that the homozygous single mutant lacking *piezo1* or *piezo2a* was viable, fertile, and did not show any developmental defect, especially in bone. Relative mRNA expression of *piezo1* and *piezo2a* in each mutant background did not change significantly, indicating transcriptional adaptation or NMD pathway is not recruited for the mechanism of genetic buffering (El-Brolosy and Stainier, 2017).

Instead of relying on transcriptional adaptation, the most likely explanation for genetic compensation in the *piezo1* null mutant is gene redundancy. This concept suggests that the loss of one gene may be compensated by another gene with overlapping functions and expression patterns (El-Brolosy and Stainier, 2017). It has been reported that *piezo1* and *piezo2a* exhibit similar expression patterns (Faucherre et al., 2013). Moreover, double knock-out mutant died after 10 dpf, while mutant harbouring at least one wildtype allele of *piezo1* or *piezo2a* (*piezo1*$^{-/-}$;*piezo2a*$^{+/-}$ or *piezo1*$^{+/-}$;*piezo2a*$^{-/-}$) showed normal phenotype and could reach adult stage. This indicates that at least one functional gene either *piezo1* or *piezo2a* is enough for normal development of zebrafish, supporting the result of gene compensation through redundant function of *piezo1* or *piezo2a* gene.

4.4 *piezo1*$^{11aa\ del/11aa\ del}$ mutant for a tool to investigate the *piezo* genes in other cells

piezo1 and *piezo2a* are homologous in function and both genes are expressed in almost all cells. Double deletion mutations cause hypoplasia in bladder and body segments as well as osteogenesis imperfecta. These results indicate that the *piezo* genes are also essential for the formation of other organs in zebrafish and are consistent with other reports showing *piezo* gene function in a variety of cells. Although 11aa del-Piezo1 is a mutation in the *piezo1* gene, it is also possible this can reduce the function of *piezo2a* with a dominant-negative effect through heteromeric channel formation (Gnanasambandam et al., 2018). This also consistent with mosaic mutant experiment (Figure 1J) when *piezo2a* function was partially reduced. This feature may allow *in vivo* studies of *piezo* genes' function in other cells. Specifically, expression of the 11aa del-Piezo1 mutant gene using a target cell-specific promoter would avoid lethality and reveal the role of the *piezo* genes in those cells.

Data availability statement

The original contributions presented in the study are included in the article/Supplementary Materials, further inquiries can be directed to the corresponding authors.

Ethics statement

The animal study was approved by Animal Experiments Committee of Osaka University. The study was conducted in accordance with the local legislation and institutional requirements.

Author contributions

Ramli: Conceptualization, Data curation, Investigation, Methodology, Visualization, Writing–original draft. TA: Conceptualization, Methodology, Supervision, Validation, Funding acquisition, Writing–review and editing. MW: Conceptualization, Methodology, Validation, Writing–review and editing. SK: Conceptualization, Funding acquisition, Investigation, Resources, Supervision, Writing–review and editing.

Funding

The author(s) declare financial support was received for the research, authorship, and/or publication of this article. This research was supported by Grant-in-Aid for Transformative Research Areas (20H05943), Grant-in-Aid for Scientific Research (19H00994), The Ministry of Education, Culture, Sports, Science and Technology (MEXT), Japan, JSPS KAKENHI Grant Number JP16K14736 and JST PRESTO JPMJPR2042.

Acknowledgments

The authors would like to thank the members of the Kondo laboratory for their experimental support and for providing valuable feedback on this study. *osx-GFP* transgenic fish was kindly gifted from Dr. Junpei Kuroda. Piezo1-deficient N2A cell was gifted from Dr. Kenta Maruyama at National Institute for Physiological Sciences & Dr. Yasunori Takayama at Showa University.

Conflict of interest

The authors declare that the research was conducted in the absence of any commercial or financial relationships that could be construed as a potential conflict of interest.

Publisher's note

All claims expressed in this article are solely those of the authors and do not necessarily represent those of their affiliated organizations, or those of the publisher, the editors and the reviewers. Any product that may be evaluated in this article, or claim that may be made by its manufacturer, is not guaranteed or endorsed by the publisher.

Supplementary material

The Supplementary Material for this article can be found online at: https://www.frontiersin.org/articles/10.3389/fgene.2023.1321379/full#supplementary-material

References

Akazawa, T., Kotani, T., Sakuma, T., Minami, S., Orita, S., Fujimoto, K., et al. (2017). Spinal fusion on adolescent idiopathic scoliosis patients with the level of L4 or lower can increase lumbar disc degeneration with sagittal imbalance 35 years after surgery. *Spine Surg. Relat. Res.* 1, 72–77. doi:10.22603/ssrr.1.2016-0017

Allam, A. M., and Schwabe, A. L. (2013). Neuromuscular scoliosis. *PM R.* 5, 957–963. doi:10.1016/j.pmrj.2013.05.015

Almomen, F. A., Altaweel, A. M., Abunadi, A. K., Hashem, A. E., Alqarni, R. M., and Alsiddiky, A. M. (2021). Determining the correlation between Cobb angle severity and bone mineral density in women with adolescent idiopathic scoliosis. *J. Taibah Univ. Med. Sci.* 16, 365–368. doi:10.1016/j.jtumed.2020.12.019

Assaraf, E., Blecher, R., Heinemann-Yerushalmi, L., Krief, S., Biton, I. E., Brumfeld, V., et al. (2020). Piezo2 expressed in proprioceptive neurons is essential for skeletal integrity. *Nat. Commun.* 11, 3168. doi:10.1038/s41467-020-16971-6

Bagwell, J., Norman, J., Ellis, K., Peskin, B., Hwang, J., Ge, X., et al. (2020). Notochord vacuoles absorb compressive bone growth during zebrafish spine formation. *Elife* 9, e51221. doi:10.7554/eLife.51221

Bearce, E. A., Irons, Z. H., O'hara-Smith, J. R., Kuhns, C. J., Fisher, S. I., Crow, W. E., et al. (2022). Urotensin II-related peptides, Urp1 and Urp2, control zebrafish spine morphology. *Elife* 11, e83883. doi:10.7554/eLife.83883

Bertram, H., Steck, E., Zimmerman, G., Chen, B., Carstens, C., Nerlich, A., et al. (2006). Accelerated intervertebral disc degeneration in scoliosis versus physiological ageing develops against a background of enhanced anabolic gene expression. *Biochem. Biophys. Res. Commun.* 342, 963–972. doi:10.1016/j.bbrc.2006.02.048

Bobyn, J. D., Little, D. G., Gray, R., and Schindeler, A. (2015). Animal models of scoliosis. *J. Orthop. Res.* 33, 458–467. doi:10.1002/jor.22797

Buglo, E., Sarmiento, E., Martuscelli, N. B., Sant, D. W., Danzi, M. C., Abrams, A. J., et al. (2020). Genetic compensation in a stable slc25a46 mutant zebrafish: a case for using F0 CRISPR mutagenesis to study phenotypes caused by inherited disease. *PLoS One* 15, e0230566. doi:10.1371/journal.pone.0230566

Burwell, R. G., Aujla, R. K., Grevitt, M. P., Dangerfield, P. H., Moulton, A., Randell, T. L., et al. (2009). Pathogenesis of adolescent idiopathic scoliosis in girls - a double neuro-osseous theory involving disharmony between two nervous systems, somatic and autonomic expressed in the spine and trunk: possible dependency on sympathetic nervous system and hormones with implications for medical therapy. *Scoliosis* 4, 24. doi:10.1186/1748-7161-4-24

Castelein, R. M., Van Dieën, J. H., and Smit, T. H. (2005). The role of dorsal shear forces in the pathogenesis of adolescent idiopathic scoliosis--a hypothesis. *Med. Hypotheses* 65, 501–508. doi:10.1016/j.mehy.2005.03.025

Chen, C., Xu, C., Zhou, T., Gao, B., Zhou, H., Zhang, C., et al. (2016). Abnormal osteogenic and chondrogenic differentiation of human mesenchymal stem cells from patients with adolescent idiopathic scoliosis in response to melatonin. *Mol. Med. Rep.* 14, 1201–1209. doi:10.3892/mmr.2016.5384

Chen, F., Sun, M., Peng, F., Lai, Y., Jiang, Z., Zhang, W., et al. (2023). Compressive stress induces spinal vertebral growth plate chondrocytes apoptosis via Piezo1. *J. Orthop. Res.* 41, 1792–1802. doi:10.1002/jor.25527

Cheng, J. C., Castelein, R. M., Chu, W. C., Danielsson, A. J., Dobbs, M. B., Grivas, T. B., et al. (2015). Adolescent idiopathic scoliosis. *Nat. Rev. Dis. Prim.* 1, 15030. doi:10.1038/nrdp.2015.30

Cheng, J. C., Tang, S. P., Guo, X., Chan, C. W., and Qin, L. (2001). Osteopenia in adolescent idiopathic scoliosis: a histomorphometric study. *Spine (Phila Pa 1976)* 26, E19–E23. doi:10.1097/00007632-200102010-00002

El-Brolosy, M. A., and Stainier, D. Y. R. (2017). Genetic compensation: a phenomenon in search of mechanisms. *PLoS Genet.* 13, e1006780. doi:10.1371/journal.pgen.1006780

Fagan, A. B., Kennaway, D. J., and Oakley, A. P. (2009). Pinealectomy in the chicken: a good model of scoliosis? *Eur. Spine J.* 18, 1154–1159. doi:10.1007/s00586-009-0927-7

Faucherre, A., Nargeot, J., Mangoni, M. E., and Jopling, C. (2013). piezo2b regulates vertebrate light touch response. *J. Neurosci.* 33, 17089–17094. doi:10.1523/JNEUROSCI.0522-13.2013

Gao, Y., Dai, Z., Shi, C., Zhai, G., Jin, X., He, J., et al. (2016). Depletion of myostatin b promotes somatic growth and Lipid metabolism in zebrafish. *Front. Endocrinol. (Lausanne)* 7, 88. doi:10.3389/fendo.2016.00088

Gnanasambandam, R., Bae, C., Ziegler, L., Sachs, F., and Gottlieb, P. A. (2018). Functional analyses of heteromeric human PIEZO1 Channels. *PLoS One* 13, e0207309. doi:10.1371/journal.pone.0207309

Gorman, K. F., and Breden, F. (2009). Idiopathic-type scoliosis is not exclusive to bipedalism. *Med. Hypotheses* 72, 348–352. doi:10.1016/j.mehy.2008.09.052

Gorman, K. F., Tredwell, S. J., and Breden, F. (2007). The mutant guppy syndrome curveback as a model for human heritable spinal curvature. *Spine (Phila Pa 1976)* 32, 735–741. doi:10.1097/01.brs.0000259081.40354.e2

Grimes, D. T., Boswell, C. W., Morante, N. F., Henkelman, R. M., Burdine, R. D., and Ciruna, B. (2016). Zebrafish models of idiopathic scoliosis link cerebrospinal fluid flow defects to spine curvature. *Science* 352, 1341–1344. doi:10.1126/science.aaf6419

Gudipaty, S. A., Lindblom, J., Loftus, P. D., Redd, M. J., Edes, K., Davey, C. F., et al. (2017). Mechanical stretch triggers rapid epithelial cell division through Piezo1. *Nature* 543, 118–121. doi:10.1038/nature21407

Guido, G., Scaglione, M., Fabbri, L., and Ceglia, M. J. (2009). The "osteoporosis disease. *Clin. Cases Min. Bone Metab.* 6, 114–116.

Haliloglu, G., Becker, K., Temucin, C., Talim, B., Küçükşahin, N., Pergande, M., et al. (2017). Recessive PIEZO2 stop mutation causes distal arthrogryposis with distal muscle weakness, scoliosis and proprioception defects. *J. Hum. Genet.* 62, 497–501. doi:10.1038/jhg.2016.153

Hawes, M. C., and O'brien, J. P. (2006). The transformation of spinal curvature into spinal deformity: pathological processes and implications for treatment. *Scoliosis* 1, 3. doi:10.1186/1748-7161-1-3

Hayes, M., Gao, X., Yu, L. X., Paria, N., Henkelman, R. M., Wise, C. A., et al. (2014). ptk7 mutant zebrafish models of congenital and idiopathic scoliosis implicate dysregulated Wnt signalling in disease. *Nat. Commun.* 5, 4777. doi:10.1038/ncomms5777

Hristova, G. I., Jarzem, P., Ouellet, J. A., Roughley, P. J., Epure, L. M., Antoniou, J., et al. (2011). Calcification in human intervertebral disc degeneration and scoliosis. *J. Orthop. Res.* 29, 1888–1895. doi:10.1002/jor.21456

Hui, S. S. C., Lau, R. W. L., Cheng, J. C. Y., and Lam, T. P. (2022). High-impact weight-bearing home exercises in girls with adolescent idiopathic scoliosis: a pilot study (abridged secondary publication). *Hong Kong Med. J.* 28 (Suppl. 3), 31–33.

Iwasaki, M., Kuroda, J., Kawakami, K., and Wada, H. (2018). Epidermal regulation of bone morphogenesis through the development and regeneration of osteoblasts in the zebrafish scale. *Dev. Biol.* 437, 105–119. doi:10.1016/j.ydbio.2018.03.005

Kague, E., Turci, F., Newman, E., Yang, Y., Brown, K. R., Aglan, M. S., et al. (2021). 3D assessment of intervertebral disc degeneration in zebrafish identifies changes in bone density that prime disc disease. *Bone Res.* 9, 39. doi:10.1038/s41413-021-00156-y

Kawakami, K., Shima, A., and Kawakami, N. (2000). Identification of a functional transposase of the Tol2 element, an Ac-like element from the Japanese medaka fish, and its transposition in the zebrafish germ lineage. *Proc. Natl. Acad. Sci. U. S. A.* 97, 11403–11408. doi:10.1073/pnas.97.21.11403

Kawamoto, T. (2003). Use of a new adhesive film for the preparation of multi-purpose fresh-frozen sections from hard tissues, whole-animals, insects and plants. *Arch. Histol. Cytol.* 66, 123–143. doi:10.1679/aohc.66.123

Konieczny, M. R., Senyurt, H., and Krauspe, R. (2013). Epidemiology of adolescent idiopathic scoliosis. *J. Child. Orthop.* 7, 3–9. doi:10.1007/s11832-012-0457-4

Kulis, A., Goździalska, A., Drąg, J., Jaśkiewicz, J., Knapik-Czajka, M., Lipik, E., et al. (2015). Participation of sex hormones in multifactorial pathogenesis of adolescent idiopathic scoliosis. *Int. Orthop.* 39, 1227–1236. doi:10.1007/s00264-015-2742-6

Lau, R. W., Cheuk, K. Y., Ng, B. K., Tam, E. M., Hung, A. L., Cheng, J. C., et al. (2021). Effects of a home-based exercise intervention (E-Fit) on bone density, muscle function, and quality of life in girls with adolescent idiopathic scoliosis (ais): a pilot randomized controlled trial. *Int. J. Environ. Res. Public Health* 18, 10899. doi:10.3390/ijerph182010899

Lee, S., Park, S., Kim, H. Y., Chae, J. H., and Ko, J. M. (2021). Extended phenotypes of PIEZO1-related lymphatic dysplasia caused by two novel compound heterozygous variants. *Eur. J. Med. Genet.* 64, 104295. doi:10.1016/j.ejmg.2021.104295

Li, X., Hung, V. W. Y., Yu, F. W. P., Hung, A. L. H., Ng, B. K. W., Cheng, J. C. Y., et al. (2020). Persistent low-normal bone mineral density in adolescent idiopathic scoliosis with different curve severity: a longitudinal study from presentation to beyond skeletal maturity and peak bone mass. *Bone* 133, 115217. doi:10.1016/j.bone.2019.115217

Li, X. F., Li, H., Liu, Z. D., and Dai, L. Y. (2008). Low bone mineral status in adolescent idiopathic scoliosis. *Eur. Spine J.* 17, 1431–1440. doi:10.1007/s00586-008-0757-z

Lv, X., Xu, J., Jiang, J., Wu, P., Tan, R., and Wang, B. (2021). Genetic animal models of scoliosis: a systematical review. *Bone* 152, 116075. doi:10.1016/j.bone.2021.116075

Marie-Hardy, L., Cantaut-Belarif, Y., Pietton, R., Slimani, L., and Pascal-Moussellard, H. (2021). Author Correction: the orthopedic characterization of cfap298^{tm304} mutants validate zebrafish to faithfully model human AIS. *Sci. Rep.* 11, 16017. doi:10.1038/s41598-021-95273-3

Murthy, S. E., Dubin, A. E., and Patapoutian, A. (2017). Piezos thrive under pressure: mechanically activated ion channels in health and disease. *Nat. Rev. Mol. Cell Biol.* 18, 771–783. doi:10.1038/nrm.2017.92

Nishida, M., Yagi, M., Suzuki, S., Takahashi, Y., Nori, S., Tsuji, O., et al. (2023). Persistent low bone mineral density in adolescent idiopathic scoliosis: a longitudinal study. *J. Orthop. Sci.* 28, 1099–1104. doi:10.1016/j.jos.2022.07.005

Park, W. W., Suh, K. T., Kim, J. I., Kim, S. J., and Lee, J. S. (2009). Decreased osteogenic differentiation of mesenchymal stem cells and reduced bone mineral density in patients with adolescent idiopathic scoliosis. *Eur. Spine J.* 18, 1920–1926. doi:10.1007/s00586-009-1129-z

Ran, F. A., Hsu, P. D., Wright, J., Agarwala, V., Scott, D. A., and Zhang, F. (2013). Genome engineering using the CRISPR-Cas9 system. *Nat. Protoc.* 8, 2281–2308. doi:10.1038/nprot.2013.143

Renn, J., and Winkler, C. (2009). Osterix-mCherry transgenic medaka for *in vivo* imaging of bone formation. *Dev. Dyn.* 238, 241–248. doi:10.1002/dvdy.21836

Sadat-Ali, M., Al-Othman, A., Bubshait, D., and Al-Dakheel, D. (2008). Does scoliosis causes low bone mass? A comparative study between siblings. *Eur. Spine J.* 17, 944–947. doi:10.1007/s00586-008-0671-4

Sarioglu, O., Gezer, S., Sarioglu, F. C., Koremezli, N., Kara, T., Akcali, O., et al. (2019). Evaluation of vertebral bone mineral density in scoliosis by using quantitative computed tomography. *Pol. J. Radiol.* 84, e131–e135. doi:10.5114/pjr.2019.84060

Schlager, B., Krump, F., Boettinger, J., Niemeyer, F., Ruf, M., Kleiner, S., et al. (2018). Characteristic morphological patterns within adolescent idiopathic scoliosis may be explained by mechanical loading. *Eur. Spine J.* 27, 2184–2191. doi:10.1007/s00586-018-5622-0

She, J., Wu, Y., Lou, B., Lodd, E., Klems, A., Schmoehl, F., et al. (2019). Genetic compensation by epob in pronephros development in epoa mutant zebrafish. *Cell Cycle* 18, 2683–2696. doi:10.1080/15384101.2019.1656019

Shea, K. G., Ford, T., Bloebaum, R. D., D'astous, J., and King, H. (2004). A comparison of the microarchitectural bone adaptations of the concave and convex thoracic spinal facets in idiopathic scoliosis. *J. Bone Jt. Surg. Am.* 86, 1000–1006. doi:10.2106/00004623-200405000-00017

Sugisawa, E., Takayama, Y., Takemura, N., Kondo, T., Hatakeyama, S., Kumagai, Y., et al. (2020). RNA sensing by gut Piezo1 is essential for systemic serotonin synthesis. *Cell* 182, 609–624. doi:10.1016/j.cell.2020.06.022

Suh, J., Kim, N. K., Lee, S. H., Eom, J. H., Lee, Y., Park, J. C., et al. (2020). GDF11 promotes osteogenesis as opposed to MSTN, and follistatin, a MSTN/GDF11 inhibitor, increases muscle mass but weakens bone. *Proc. Natl. Acad. Sci. U. S. A.* 117, 4910–4920. doi:10.1073/pnas.1916034117

Sun, W., Chi, S., Li, Y., Ling, S., Tan, Y., Xu, Y., et al. (2019). The mechanosensitive Piezo1 channel is required for bone formation. *Elife* 8, e47454. doi:10.7554/eLife.47454

Troutwine, B. R., Gontarz, P., Konjikusic, M. J., Minowa, R., Monstad-Rios, A., Sepich, D. S., et al. (2020). The reissner fiber is highly dynamic *in vivo* and controls morphogenesis of the spine. *Curr. Biol.* 30, 2353–2362. doi:10.1016/j.cub.2020.04.015

Uehara, M., Kosho, T., Takano, K., Inaba, Y., Kuraishi, S., Ikegami, S., et al. (2020). Proximal junctional kyphosis after posterior spinal fusion for severe kyphoscoliosis in a patient with PIEZO2-deficient arthrogryposis syndrome. *Spine (Phila Pa 1976)* 45, E600–E604. doi:10.1097/BRS.0000000000003347

Welle, S., Bhatt, K., Pinkert, C. A., Tawil, R., and Thornton, C. A. (2007). Muscle growth after postdevelopmental myostatin gene knockout. *Am. J. Physiol. Endocrinol. Metab.* 292, E985–E991. doi:10.1152/ajpendo.00531.2006

Whittle, J., Antunes, L., Harris, M., Upshaw, Z., Sepich, D. S., Johnson, A. N., et al. (2020). MYH3-associated distal arthrogryposis zebrafish model is normalized with para-aminoblebbistatin. *EMBO Mol. Med.* 12, e12356. doi:10.15252/emmm.202012356

Wise, C. A., Gao, X., Shoemaker, S., Gordon, D., and Herring, J. A. (2008). Understanding genetic factors in idiopathic scoliosis, a complex disease of childhood. *Curr. Genomics* 9, 51–59. doi:10.2174/138920208783884874

Wu, Z., Zhu, X., Xu, L., Liu, Z., Feng, Z., Hung, V. W. Y., et al. (2023). More prevalent and severe low bone-mineral density in boys with severe adolescent idiopathic scoliosis than girls: a retrospective study of 798 surgical patients. *J. Clin. Med.* 12, 2991. doi:10.3390/jcm12082991

Xie, H., Li, M., Kang, Y., Zhang, J., and Zhao, C. (2022). Zebrafish: an important model for understanding scoliosis. *Cell Mol. Life Sci.* 79, 506. doi:10.1007/s00018-022-04534-5

Zhang, X., Jia, S., Chen, Z., Chong, Y. L., Xie, H., Feng, D., et al. (2018). Cilia-driven cerebrospinal fluid flow directs expression of urotensin neuropeptides to straighten the vertebrate body axis. *Nat. Genet.* 50, 1666–1673. doi:10.1038/s41588-018-0260-3

Zhu, D., Zhang, G., Guo, X., Wang, Y., Liu, M., and Kang, X. (2021). A new hope in spinal degenerative diseases: piezo1. *Biomed. Res. Int.* 2021, 6645193. doi:10.1155/2021/6645193